Journal of Geography & Natural Disasters
ISSN: 2167-0587
Lee et al., J Geogr Nat Disast 2016, 6:2
DOI: 10.4172/2167-0587.1000169
Research Article Open Access

Consideration of the Maximum Impact Force Design for the Rock-Shed Slab

Chia-Ming Lo[1], Ching-Fang Lee[2]* and Ming-Lang Lin[3]

[1]Department of Civil and Disaster Prevention Engineering, National United University, Miaoli, Taiwan
[2]Disaster Prevention Technology Research Center, Sinotech Engineering Consultants, INC, Taipei, Taiwan
[3]Department of Geosciences, National Taiwan University, Taipei, Taiwan

Abstract

This study aims at the estimation of the maximum impact force for a rock-shed slab under collision by a rock fall. A DEM program calibrated from small-scale physical experiments is used to model the movement of rock fall clusters and to measure the resultant impact forces. The results obtained from the small-scale experiments show that the maximum impact forces are significantly affected by the mass of the rock fall, the height from which they fall as well as the falling process. Full-scale numerical modeling based upon a field case not only confirms the experimental results but also sheds light upon the influence of the rock fall mode and the contact stiffness between the rock and the rock-shed. This study provides guidelines for the design of rock-shed structures countering large rock fall problems.

Keywords: Maximum impact force; Rock-shed slab; Physical experiment; Numerical modelling

Introduction

Rock fall disasters occur frequently in the mountainous areas of Taiwan triggered by earthquake and storm events. Falling rocks have been known to strike vehicles, demolish roads, and cause accidents. Rock-sheds, reinforced concrete structures covered with cushioning material to absorb the direct impact force, are often constructed in order to mitigate the damage caused by rock falls and to stabilize slopes prone to rock falls and avalanches. However, large quantities of rock can produce great impact which may ultimately exceed the load-bearing capacity of the rock-shed and even punch through the top slab or destroy the beam-column system.

For example, some rock-sheds along Taiwan's Central Cross-Island Highway were severely damaged by rock fall events during the Chi-Chi Earthquake. The Malin No. 3 rock-shed, located to the west of the Malin No. 3 tunnel on the Central Cross-island Highway at Taichung City, Taiwan (from 40k+866 to 40k+925), is one such case. Figure 1a shows the rock mass with the potential to form rock falls (because of several joint sets) above the Malin NO. 3 rock-shed. The rock-shed has the approximate dimensions of 70 m long, 8 m wide, and 8 m high with tires covering the roof to absorb the impact force from falling rocks. The cluster of rock falls during the Chi-Chi earthquake caused severe damage to the columns of the rock-shed and blocked traffic on the road (Figure 1b). A comparison of the topographic maps and aerial photographs shows that the height from the crest of the slope to the river valley is about 320 m. The rock fall source area is about 120 m upslope from the rock-shed. There is a talus deposit about 150 m long, 90 m wide, and 70 m high that originated from a cliff about 120 m above the rock-shed. The rock on the cliff first slid along a gentle sliding surface and then began to fall because of topographic variation, causing severe damage when striking the rock-shed. Different types of rock falls would produce different maximum impact forces and thus different levels of damage to the rock-sheds. In addition, the stiffness of the top slab and the cushioning material would also affect the maximum impact force. These issues are discussed in this study.

In recent years, there has been a dramatic increase in research regarding the process of rock falls impacts on the upper slab of a rock-shed. Numerous field experiments have been conducted to reveal the behavior of reinforced concrete structures with cushioning layers under vertical rock falls impact [1-3]. For example, Chuman et al. Ong et al. and Ebeltoft et al. [4,5] investigated single block falls in physical model experiments. In addition, single rock falls impacts on the top slab of a rock-shed have been simulated using the finite element method (Philippe et al., 2003; Delhomme et al., 2005) and the discrete element method. However, general rock falls movements can include the collision and spreading behavior of many clusters of falling rock blocks. Okura [6] provided an extensive discussion of the relation between the volume of the falling blocks, the collision interaction, and the run out distance. The fall of a single rock mass or several in sequences as well as the level of disintegration all have an influence on the impact forces on the rock-shed. Therefore, this study discusses the maximum impact force on a rock-shed induced by various types of falling in a cluster of rock falls. The numerical discrete element method (DEM) program-particle flow code (PFC) 3D [7] calibrated with a simplified analytical solution and small-scale physical modeling tests is used to investigate the maximum impact force. The developed numerical method will then be further applied to a field full-scale case study, i.e., the Malin rock-shed.

This paper investigates three types of rock falls (Figure 2): (a) the single fall (SF) where a single block of rock falls from a cliff before rolling and bouncing down a slope; (b) the cluster fall (CF) where a cluster of rock blocks falls simultaneously, which is the most common type of rock falls, including free falling, rolling, bouncing, and collision between rock fragments; and (c) the sub-cluster fall in sequence (SCSF) where multiple clusters of rock blocks (separated by joint sets) fall in sequence. The cracking process during collision is not taken into account. The remainder of this paper comprises three parts. First, the

***Corresponding author:** Ching-Fang Lee, Disaster Prevention Technology Research Center, Sinotech Engineering Consultants, INC, Taipei, Taiwan, Tel: 886-2- 27580568; E-mail: cflee@sinotech.org.tw

Received March 17, 2016; **Accepted** May 23, 2016; **Published** May 25, 2016

Citation: Lo CM, Lee CF, Lin ML (2016) Consideration of the Maximum Impact Force Design for the Rock-Shed Slab. J Geogr Nat Disast 6: 169. doi:10.4172/2167-0587.1000169

Copyright: © 2016 Lee CF, et al. This is an open-access article distributed under the terms of the Creative Commons Attribution License, which permits unrestricted use, distribution, and reproduction in any medium, provided the original author and source are credited.

Citation: Lo CM, Lee CF, Lin ML (2016) Consideration of the Maximum Impact Force Design for the Rock-Shed Slab. J Geogr Nat Disast 6: 169. doi:10.4172/2167-0587.1000169

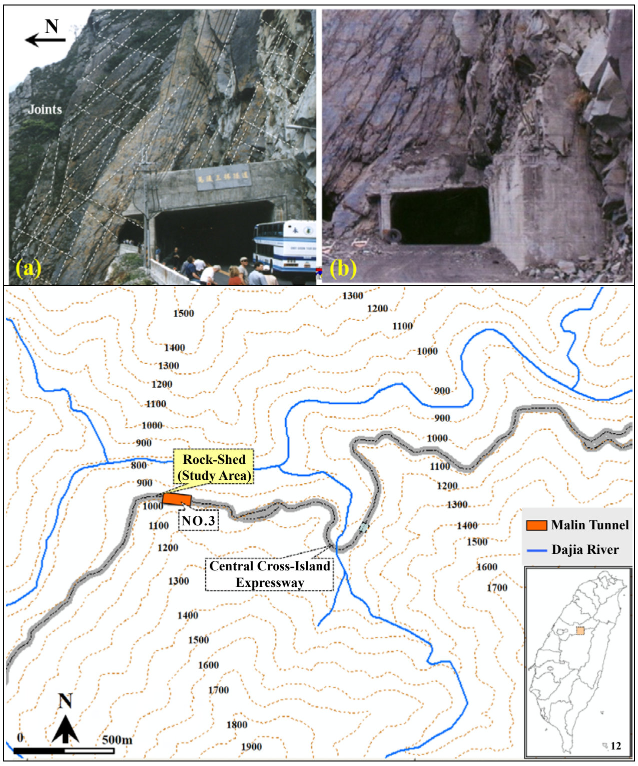

Figure 1: Malin rock-shed damaged by a rockfall induced by the Chi-chi earthquake (Modified from Lo and Chang, 2015); (a) Before the Chi-chi earthquake: large rock mass with several sets of joints above the Malin No. 3 rock-shed; (b) After the Chi-chi earthquake: the large rockfall severely damaged the column of the rock-shed and hindered traffic; (c) Topographic map at the study area (the No. 3 Malin rock-shed).

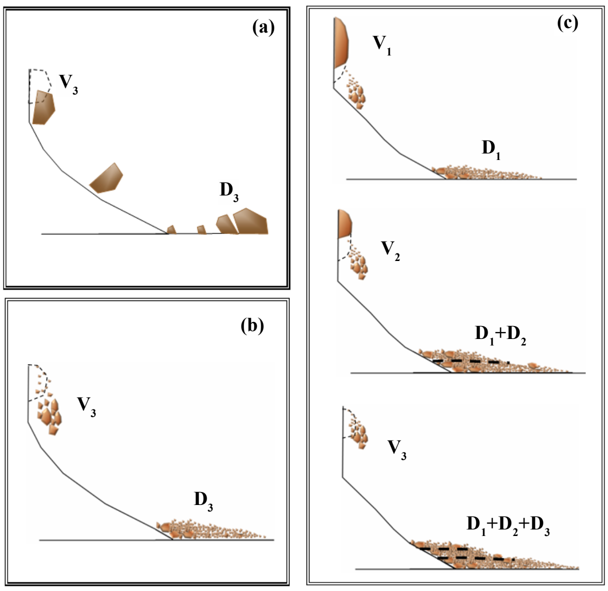

Figure 2: Illustration of rockfall type: (a) single fall (SF); (b) cluster fall (CF); (c) sub-cluster in sequence fall (SCSF).

relations between the rock falls mass, drop height, contact stiffness, and the maximum impact force are discussed. Second, the maximum impact forces with different types of rock falls are compared. Third, a field case is studied considering the influences of the type of rock falls and the contact stiffness between the rock and the rock-shed.

Methodology

Due to the scaling effect problem, a small-scale model may differ from the actual rock falls behavior. Therefore, the qualitative analyses of physical modeling tests were conducted to establish the relation models in study area. Undeniably, a full-scale model would be the best method for analysis of rock falls impact force but are far too costly and difficult to execute. In recent years, we witnessed an increase in innovative numerical approaches to the study of full-scale landslide simulation. However, to ensure that a numerical model could reveal reasonable predictions, the physical modeling tests and numerical analysis adopted must cross math with each other. The results of physical modeling were compared with those produced by numerical analysis so that the correctness of the numerical simulation could be justified. Subsequently, calibrated numerical methods adopted in the small-scale model were used to simulate the full-scale model. The simulation results should be as close to reality as much as possible.

A flowchart of this research process is shown in Figure 3. First, an analytical solution is derived showing an estimation of the maximum impact force of a single elastic ball of rock on a flat elastic ground. Meanwhile, small-scale models based on the physical modeling experiments are established using a numerical method to simulate the maximum impact force. The results obtained from the analytical solution, physical experiments and numerical methods are compared. A small-scale numerical model is calibrated based on the physical modeling experiments (Step 1 and step 2 in Figure 3) which is subsequently applied to a full-scale numerical model for estimating the maximum impact force on the Malin rock-shed of rock falls event induced during the Chi-Chi Earthquake (Step 3 in Figure 3). Factors related to the maximum impact force, including the rock falls process, amount of falling rock, and the contact stiffness between the falling rock and the rock-shed are also investigated (Step 4 in Figure 3).

Derivation of the maximum impact force

When a falling rock directly collides with the top of a rock-shed, the maximum impact force generated at that moment is much larger the weight of the rock itself and thus causes great damage. The maximum impact force under specified conditions is derived based on the following basic assumptions:

(a) The problem is simplified as a rock ball vertically colliding with a spring system, which represents the top slab of the rock-shed.

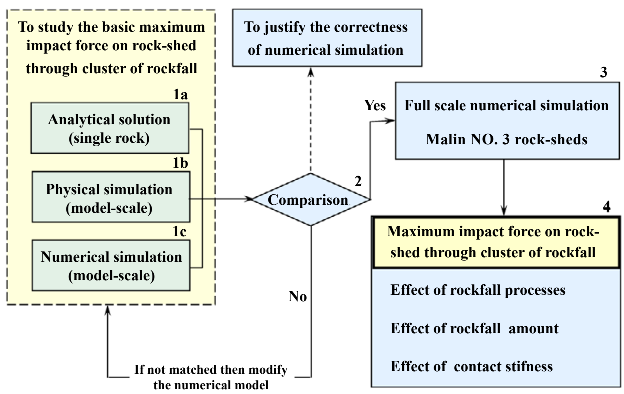

Figure 3: Flowchart of the research framework.

Citation: Lo CM, Lee CF, Lin ML (2016) Consideration of the Maximum Impact Force Design for the Rock-Shed Slab. J Geogr Nat Disast 6: 169. doi:10.4172/2167-0587.1000169

The mass of the rock ball is M, while the mass of the spring system is neglected. The stiffness of the rock ball and the rock shed are k_1 and k_2, which are assumed to be constants and independent on deformation.

(b) The collision between the rock and the rock shed causes only deformation and no fracturing or breakage. The gravitational potential energy is equal to the elastic strain energy.

(c) The maximum impact force appears to be accompanied by the maximum deformation.

According to Newton's second law of motion, the impact force of a falling object on a surface may be determined as the change of momentum in a time interval. However, it is difficult to measure the velocity of an object before and after a collision in a certain time interval. An alternative is to consider the transformation of energy from gravitational potential energy to strain energy (Figure 4). When an object with mass M released from a height H hits the spring, the deformations of the falling object and the spring are u_1 and u_2, respectively. The stiffness of the falling object and the spring are assumed to be constants k_1 and k_2. The potential energy released at the maximum deformation of the system is

$$U = Mg(H + (u_1 + u_2)) = Mg\left[H + \mathrm{F}\frac{(k_1 + k_2)}{(k_1 \cdot k_2)} \right], \quad (1)$$

where F is the maximum impact force; $\frac{k_1 \cdot k_2}{k_1 + k_2}$ is the contact stiffness of the system. The elastic strain energy at the maximum deformation of the system is

$$U_{elastic} = \frac{1}{2} \times F \times (u_1 + u_2) = F^2 \frac{(k_1 + k_2)}{2(k_1 \cdot k_2)}. \quad (2)$$

By equating (1) with (2), we obtain

$$F = Mg + Mg\sqrt{1 + \frac{2H(k_1 \cdot k_2)}{Mg(k_1 + k_2)}}. \quad (3)$$

If M, H, and k_1 are considered as constant, the contact stiffness and the maximum impact force are reduced as the stiffness of the rock-shed (k_2) decreases. As the stiffness of the rock-shed is much less than the stiffness of the rock, the contact stiffness of the system approximates the stiffness of the rock-shed.

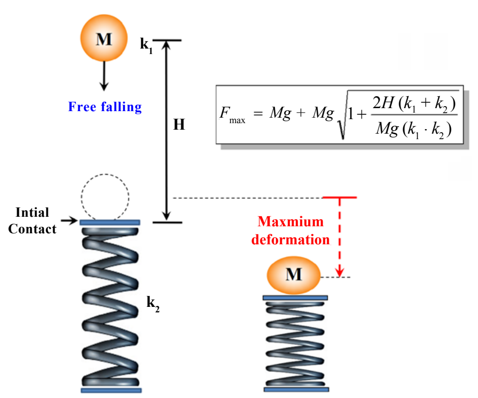

Figure 4: Derivation of maximum impact force, mass, elastic contact, and falling height. (F_{max} is the maximum impact force, M is the mass, H is the drop height, k_1 is the stiffness of the rockfall, and k_2 is the stiffness of the spring system.).

Simplified physical modeling tests

In this work, the analytical solution is compared with the test results of a single falling rock block. Then, maximum impact forces for different types of rock falls are compared. These test results are also utilized for calibration of the numerical modeling. The equipment used consists of a release container, an impact tester, and a measurement apparatus (CCD). The release container is a vertical tube 5.5 cm in diameter and 39 cm high. The impact tester is located below the release container and is composed of a platform fixed on a sensitive spring scale (Figure 5).

Tests are carried out with various rock masses and different heights to represent different types of rock falls. As the falling rock hits the platform of the impact tester, the force of the impact is measured and appears on the spring scale. Two CCD cameras capable of taking photographs at a rate of up to 30 frames per second are used to capture images of the impact. Spherical rocks and granular pieces of gravel are used in the three types of rock falls tests. The contact stiffness of the system is dominated by the stiffness of the scale because of the much greater stiffness of the rock than that of the scale.

Numerical modeling

Numerical modeling is carried out using a three-dimensional discrete element program, PFC3D (Particle Flow Code) [8]. The basic principles and related parameters used in PFC3D such as material density, stiffness (k_n and k_s), friction coefficient (μ) and damping ratio (D_n and D_s) are described below.

Basic principles of PFC3D: PFC was implemented through the development of the DEM proposed by Cundall and Strack [9]. This technique is commonly used for the modelling of granular assemblages with purely frictional or bonded circular particles represented by discs in two dimensions. The original version of the DEM was devoted to the modelling of rock-block systems; it was later applied to the modelling

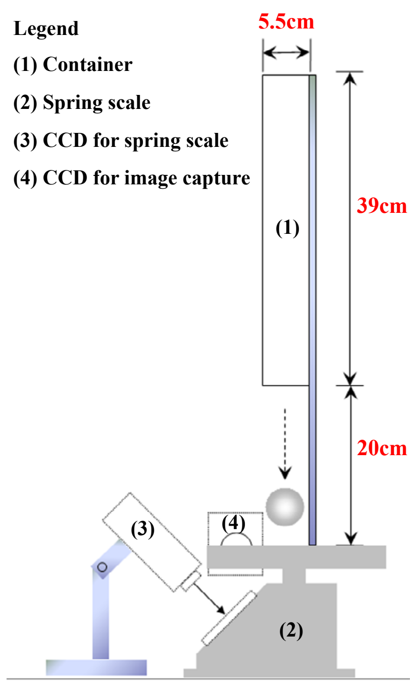

Figure 5: Experimental set-up for physical modeling.

of granular material. With this method, the global behaviour of an assembly of particles connected by a network of contacts is obtained by satisfying the equations of motion of each component for the whole particle set.

In the explicit finite difference method, the system variations of the operation process are controlled through the force-displacement relations. Beginning with the calculation of the particle position, the adjacent overlap and the relative displacement, PFC determines the contact force on the basis of the force-displacement relations. The particle velocity and up-to-date position are derived from Newton's 2nd low of motion. In general, the fundamental assumptions for the PFC model are as follows: (a) each element is considered a rigid body and a perfect sphere. By means of the combination command "Clump", particles can be formed in various shapes composed of different amount of elements; (b) PFC allows adjacent particles to overlap. The extent of overlap is related to the contact force and stiffness of particles calculated based on the force-displacement relations; (c) the strength of the bond between two particles is exhibited through contact or parallel bonds.

In PFC3D, the parameter of viscous damping, in contrast to the numerical damping factor influences the motion of the particles and reflects energy loss during collisions. Equation (4) expresses the relation between the restitution coefficient (r) and the critical damping ratio (D) observed in drop tests, and are used to estimate the critical damping ratio (D) in rock falls collisions in the laboratory or in the field.

$$D = \sqrt{\frac{(\ln(r))^2}{(\pi)^2 + (\ln(r))^2}} \qquad (4)$$

Model parameters: The macroscopic behaviour of a granular media depends on the mechanical properties of the contact between the particles, but there is no straightforward solution to the selection of these parameters. PFC models are reliable simulation tools, but it is necessary to establish reasonable relationships between the numerical parameters and the mechanical characteristics of real problems [8]. The parameters used for modeling in the physical experiments and for the case study for the Malin rock-shed are explained in the following sections.

The parameters of the physical modelling: In the numerical simulations, the area of impact and release container is modeled as planar wall elements and the spherical rocks as ball elements. The container has a radius of 0.055 m and a height of 0.39 m. The rocks are released from the height of 0.2 m. The impact area is 0.35 m by 0.35 m (Table 1). The unit weight of the rocks is 2600 kg/m^3. Comparing the results from numerical and laboratory uniaxial tests (Figure 6), we obtain the stiffness of the rock balls which is 2×10^8 to 3×10^8 N/m^2. Through conversion of the particle stiffness and macroscopic elastic modulus relations, the elastic modulus (E as 5.34 Mpa) obtained from uniaxial compression tests will lead to the stiffness of the rock (ball) as 2×10^8 to 3×10^8 N/m^2 (Table 2) and the stiffness of the impact area (wall) including both the impact tester and the scale is 8×10^7 N/m^2. The friction coefficients (μ) between the particles and particle-wall contact are determined to be 0.6 and 0.84, respectively, which are equivalent to friction angles of 31° and 40°. The normal and tangential damping ratios are 0.3 and 0.05 as calibrated using the coefficients of restitution obtained from the experimental CCD recording data. In addition, the fall heights of SF and CF as 39.5 cm, while the fall heights of SCSF as 24.9 cm (first time), 34.6 cm (second time), 44.4 cm (third time), 54.5 cm (fourth time) respectively. The volumes of SF and CF as 337 cm^3, while the volumes of SCSF as 84.25 cm^3 for each time (Table 2).

The parameters of the case study: In the case study, the upper slab of the rock-shed and the topography are modeled by planar wall elements. The impact forces from the collision of the rock falls with the wall element are measured in the X, Y, and Z directions. The rock mass is modeled as an assembly of bonded ball elements filling up the volume of the source area. The same parameters are used as in the rock fall tests except that the friction coefficients between the particles and the particle-wall contact are determined to be 0.78 assuming a general repose angle for the field talus ranging from 31° to 40°. The damping coefficients for the case study, which are listed in Table 3 are estimated using Equation (4) and the results of restitution coefficient tests in the field taken from Giani [10]. In addition, the stiffness and thickness are considered when studying the efficiency of the dissipation cushion in this case. The dissipation cushion is modeled as a cluster of ball elements 0.5 m in radius with varied dimensions of 7 × 41 × 2, 7 × 41 × 6, 7 × 41 × 10, 7 × 41 × 14, and 7 × 41 × 9. The stiffness of the dissipation cushion is determined to be 1.0E+4 kN/m^2. In addition, the fall heights of SF and CF as 120 m, while the fall heights of SCSF as 104 m (first time), 112 m (second time), 120 m (third time), 128 m (fourth time), 136 m (fifth time) respectively. The volumes of SF and CF as 28,000 m^3, while the volumes of SCSF as 5,600 m^3 for each time (Table 2).

Results of Physical Experiments and Numerical Modeling

Maximum impact of a single rock falls

The factors influencing the maximum force of impact include the

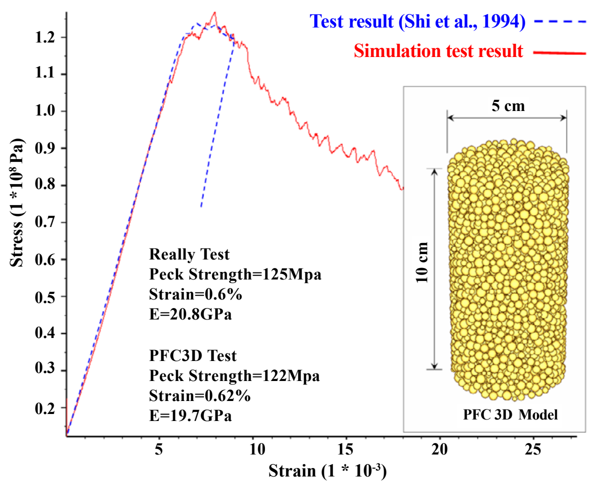

Figure 6: Simulation results of uniaxial compressive test.

	Physical experimental model	Case study (Malin rock-shed)
Source area dimensions	Radius × Height: 0.055 m × 0.39 m Fall height: 0.2 m	Length × Width × Height: 60 m × 30 m × 10 m Fall height: 120 m
Impact area dimensions	Length × Width: 0.35 m × 0.35 m	Length × Width: 70 m × 8 m

Table 1: Dimensions of the physical model and PFC case study models.

	Physical experimental model	Case study (Malin rock-shed)
Particle density	2600 kg/m³	2500 kg/m³
Stiffness of rock	Normal: 2.0×10^8 ~3.0×10^8 N/m Tangent: 2.0×10^8 ~3.0×10^8 N/m	Normal: 1.0×10^{11} ~2.0×10^{11} N/m Tangent: 1.0×10^{11} ~2.0×10^{11} N/m
Contact bonds		Normal: 2.5×10^6 ~5.0×10^6 N Tangent: 2.5×10^6 ~5.0×10^6 N
Parallel bonds		Normal stiffness: 1.4×10^{10} N/m³ Normal strength: 1.25×10^7 N/m² Tangential stiffness: 1.4×10^{10} N/m³ Tangential strength: 6.25×10^6 N/m²
Stiffness of wall	Normal: 8×10^7 N/m Tangent: 8×10^7 N/m	Normal: 2.5×10^{11} N/m Tangent: 2.5×10^{11} N/m
Friction coefficient of rock	Ball elements: 0.6 Wall elements: 0.84	Ball elements: 0.78 Wall elements: 0.78
Damping ratio	Normal: 0.3 Tangent: 0.05	Normal: 0.32 Tangent: 0.05
Single fall (SF)	Fall height: 39.5 cm Volume: 337 cm³	Fall height: 120 m Volume: 28,000 m³
Cluster fall (CF)	Fall height: 39.5 cm Volume: 337 cm³	Fall height: 120 m Volume: 28,000 m³
Sub-cluster in sequence fall (SCSF)	Fall height: 24.9 cm (first time), 34.6 cm (second time), 44.4 cm (third time), 54.5 cm (fourth time) Volume: 84.25 cm³ (each time)	Fall height: 104 m (first time), 112 m (second time), 120 m (third time), 128 m (fourth time) , 136 m (fifth time) Volume: 5,600 m³ (each time)

Table 2: The parameters of PFC models.

Slope materials	Normal restitution coefficient (Rn)	Damping ratio	Shear restitution coefficient (Rt)	Damping ratio
Bedrock	0.50	0.21	0.95	0.02
Bedrock covered by large blocks	0.35	0.32	0.85	0.05
Debris formed by uniform distributed elements	0.30	0.36	0.70	0.11
Soil covered vegetation	0.25	0.40	0.55	0.20

Table 3: Relation between restitution coefficients and damping ratios in rockfall tests in the field (modified from Giani, 1992).

rock mass, the drop height, and the contact stiffness between colliding objects. Figure 7 shows the normalized relations between the maximum impact force and the effect of the drop height and contact stiffness. A comparison of the results from laboratory tests and the case study for the Central Cross-island Highway in Taiwan is shown in Figure 7.

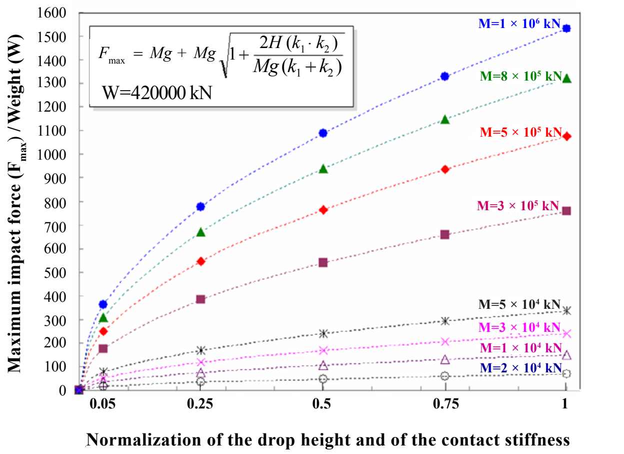

Figure 7: Comparison of maximum impact force (analytical solution) based on the mass, drop height, and contact stiffness. The maximum drop height is 200 m is used as the divisor of normalization; the maximum contact stiffness is 1×10^8 kN/m and is used as the divisor of normalization.

The maximum impact forces from a single and a cluster of rock falls

The maximum impact forces for different weights of rock falls but the same drop height of 0.2 m are shown in Figure 8 and Table 4, including the results from the analytical solution, experiments, and numerical modeling. In the single rock falls tests, the spherical rocks have weights of 0.25 N, 0.65 N, and 1.5 N, the same gross weight as a cluster of small size gravel. The impact forces generated by rock falls clusters (3.2 N, 5.3 N, 8.3 N) are clearly less than those of a single rock falls (2.9 N, 4.8 N, 7.3 N). This trend is more significant as the weight of the rock falls becomes greater.

Numerical modeling

As shown in Figure 8, the maximum impact forces of a single rock falls or clusters of rock falls are estimated in the numerical modeling. The process includes placing rock elements in the container, releasing them, free fall, colliding the slab, and successive deposition of talus (Figure 9). The variations of the impact forces are measured and recorded.

Comparison of experimental results with varied types of rock falls

Figure 10 shows the maximum impact forces for different clusters of rock falls. The greatest force is generated by the dropping of the 10 N clusters. Clusters with the same gross weight are dropped successively four times from different heights, denoted A, B, C and D. Even though the drop height is greater, the second drop generates less impact because the deposit from the first drop acts as a cushion. Then, for the third and fourth drops, the greater the drop height, the greater the maximum impact force.

Case Study of the Malin No. 3 Rock-shed

A numerical method is used to study the case of the Malin

Citation: Lo CM, Lee CF, Lin ML (2016) Consideration of the Maximum Impact Force Design for the Rock-Shed Slab. J Geogr Nat Disast 6: 169. doi:10.4172/2167-0587.1000169

No. 3 rock-shed located on the Central Cross-island Highway between 40k+866 and 40k+925 (Figure 1c). During the 1999 Chi-Chi Earthquake, this rock-shed was destroyed by rock falls; the surrounding rock mass with several sets of joints is shown in Figure 1 and Figure 11b. Interpretation of aerial photographs from 1998 and 1999, topographic analysis and field reconnaissance shows the height of rock falls to be around 120 m (Figure 11a).

Measurements of several cases of rock falls on the Central Cross-island Highway show the rock masses to have fallen from heights 50 m to 300 m with volumes from 1000 m^3 to 50000 m^3. Before it was destroyed, there was a layer of tires on top of the Malin No. 3 rock-shed 0.5 m thick. Numerical modeling is used to investigate the effects of the rock joint spacing, type of rock falls, material stiffness of the slab, and thickness of the cushion on the maximum impact force generated by rock falls clusters. The results are helpful to evaluation of the maximum impact force and the design of rock-shed structures.

Numerical modeling

The results of aerial photograph interpretation and topographic analysis show the area of the rock falls to be 56 m in length, 30 m in width and 10 m in height after falling about 120 m. In the model the top slab of the rock-shed is about 70 m long and 8 m wide (Table 1 and Figure 12). Joints in the rock around the Maline No. 3 rock-shed are analyzed based on the interpretation of aerial photos from 1998 to 2006. Two joint sets orientated N80°W/75° NE (Joint A obtained from 13 data sets) and N10°E/85° NW (Joint B obtained from 19 data sets) are modeled in three dimensions (Figure 11c). The modeling process includes three steps. First, the initial state of the rock mass in the source area is modeled. Second, a cluster of rocks separate from the source area and slide under the influence of gravity without considering the effects of earthquake or rainfall. Third, the rocks slide over a convex point where the inclination of the slope changes from 30° to 65° and then strike the roof slab of the rock-shed. The factors discussed herein for calculating the maximum impact forces include the type of rock falls, joint spacing (1 m, 4 m, 7 m, and 10 m), slab stiffness (1×10^5, 1×10^6, 1×10^7, and 1×10^9 KN/m), and the thickness of the dissipation cushion (1 m, 3 m, 5 m, 7 m, and 9 m).

Results of the case study

The force of the maximum impact on the rock-shed is influenced by the factors discussed below.

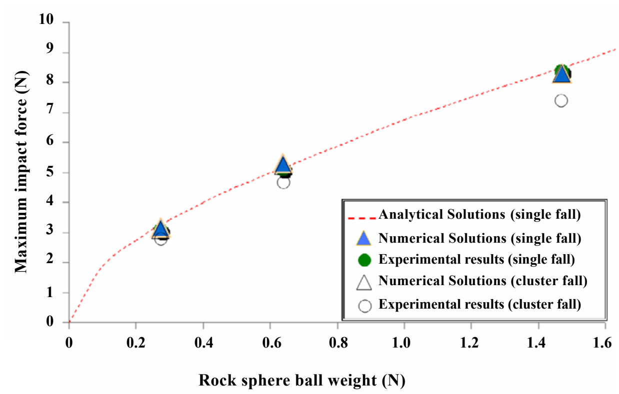

Figure 8: Comparison of maximum impact force transmitted by releasing rock spheres with different masses.

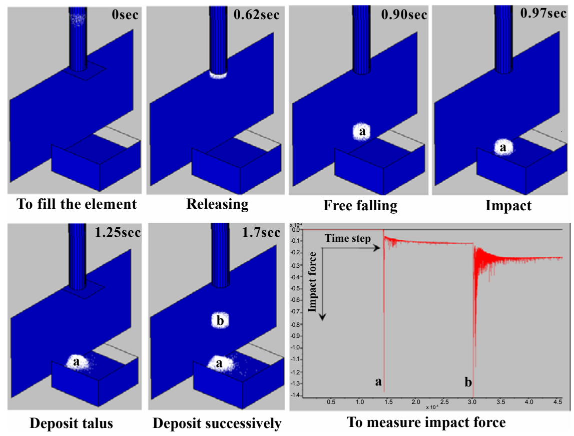

Figure 9: Simulation results from PFC models.

Experimental items \ Discussion items			Maximum impact force (N)	Error (%)	Remarks
Single fall	Analytical solution	0.25 N	3.25	--	Analytical solutions are the baseline values
		0.65 N	5.10	--	
		1.5 N	8.49	--	
	Experimental results	0.25 N	3.04	6.49%	
		0.65 N	5.00	1.89%	
		1.5 N	8.34	1.78%	
	Numerical solution	0.25 N	3.17	2.57%	
		0.65 N	5.20	1.88%	
		1.5 N	8.30	2.24%	
Cluster fall	Experimental results	0.25 N	2.81	--	Experimental results are the baseline values
		0.65 N	4.72	--	
		1.5 N	7.36	--	
	Numerical solution	0.25 N	3.00	6.83%	
		0.65 N	5.13	8.67%	
		1.5 N	8.21	11.60%	
Error (%)=(Baseline values – Test group)/Baseline values					

Table 4: Analytical, experimental, numerical solution and error analysis results.

Citation: Lo CM, Lee CF, Lin ML (2016) Consideration of the Maximum Impact Force Design for the Rock-Shed Slab. J Geogr Nat Disast 6: 169. doi:10.4172/2167-0587.1000169

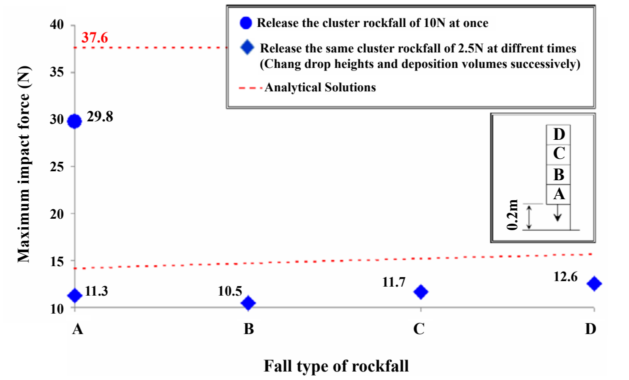

Figure 10: Comparison of maximum impact force transmitted by releasing a single rock, or clusters of rock at once and at different times.

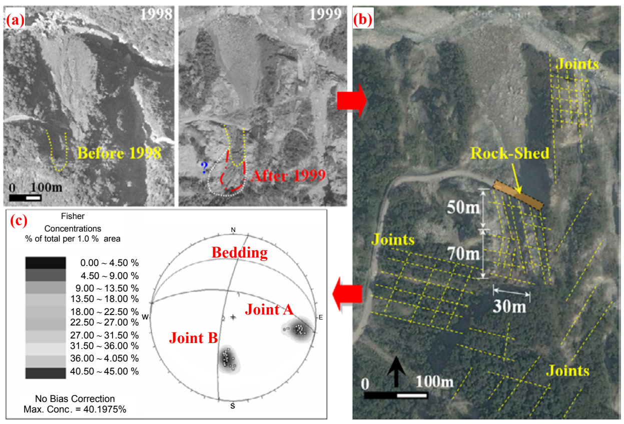

Figure 11: Potential rock-falls and orientation of joints above the No. 3 Malin tunnel rock-shed. (a): A comparison of 1998 and 1999 aerial photographs, showing the Malin No.3 rock-shed located in the west of Malin No. 3 tunnel. Large rockfalls caused severe damage to the rock-shed after the Chi-Chi earthquake. The red dotted line on the right indicates the expanded range of the cliff (rockfall source area) from 1998 to 1999. (b-c): Rocky outcrops from aerial photos from 1998 to 2006 of the Malin No. 3 rock-shed, with two sets of joints found and analyzed by the Dip 5.0 software. Joint A (13 outcrops, joint spacing as about 1 m) and Joint B (19 outcrops, joint spacing as about 4-9 m) are respectively oriented N80°W/75°NE and N10°E/85°NW; the orientation for the bed is N80°W/30°NE.

(1) Types of rock falls

The type of rock falls is critically important to laying the groundwork for understanding how civil engineers can decrease the maximum force of impact and thus the danger of damage. Three types of rock falls are illustrated in Figure 13a-13c. A single huge rock falling directly onto a slab will cause more serious damage than a cluster of falling rocks. The maximum impact of a single rock falling without sliding, as calculated from the analytical solution, is about 1474 times the magnitude of the weight of the falling rock. On the other hand, the maximum impact force of a single rock falling from a convex slope after sliding is only about 974 times the magnitude of the weight of the falling rock. The maximum impact force generated by a cluster of falling rock separated with a joint spacing of 4 m is 191 times the magnitude of weight of the rock, whereas a cluster of debris falling at the same time (with dimensions of about 0.1 m-0.5 m) generates a smaller maximum impact force (Figure 14 and Table 5).

An examination of Figure 15 shows that the maximum impact force generated by a cluster of falling rock is larger than that generated by sub-clusters falling in sequence. The greater the separation in the sequence, the less the maximum impact force generated, although there is only a very slight change in the maximum impact force when the sub-cluster in the rock falls sequence is separated along a 4 m joint spacing at four times and the sub-cluster in sequence debris fall at twice respectively. The results indicate that the maximum impact force is affected by the viscous and plastic behavior of a cluster of rock and by the rock falls process. Thus if there is danger of a huge rock that

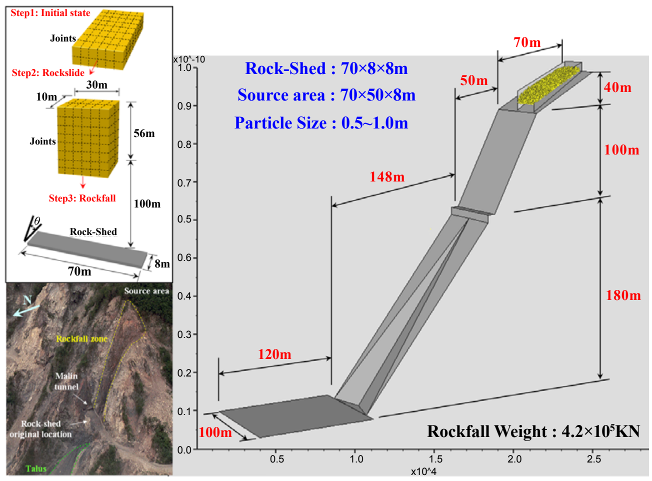

Figure 12: Configuration of the case study.

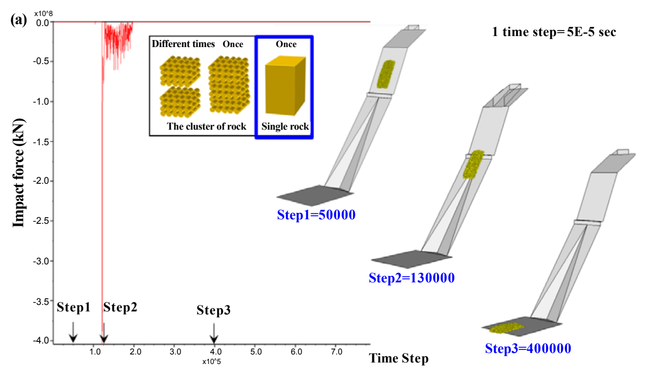

Figure 13a: Impact processes in case study simulated by SF models.

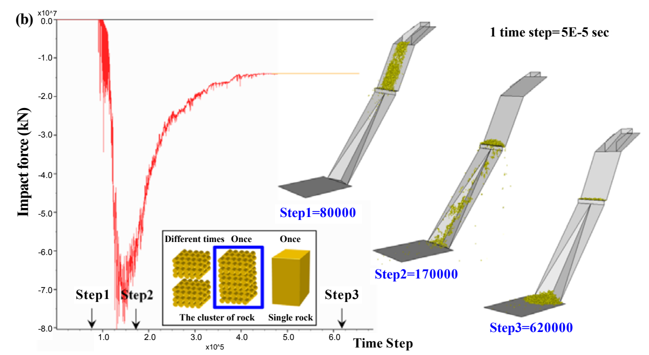

Figure 13b: Impact processes in case study simulated by CF models.

threatens a lower rock-shed, it may be appropriate to first explore the surrounding situation. It could be preferable to blast the rocky mass to break it up and let it fall in sequence rather than all at once.

(2) Joint spacing of the rock mass

Rock falls source areas are often rocky masses with fractures, or slopes with undercuts where the matrix has been destroyed. Discontinuities in the rock mass are relevant to rock fall problems [11-16]. An examination of Figure 16 shows that the maximum impact forces of a cluster of rock falls are influenced by the joint spacing. The force of the maximum impact increases as the joint spacing increases past 4 m. The results also indicate that when a rock mass has the same volume but is more fragmented, the influence of the collision interaction will be more significant, although the influence of the mass and the drop height still need to be considered.

(3) Stiffness of the top slab of a rock-shed

One common design guideline is to change the stiffness of the slab by varying the material stiffness. The maximum impact force decreases as the stiffness of the slab decreases. In this case study, when the stiffness is lowered by 1×10^{-3} times, the maximum impact fore will be reduced to 1.7 times (Figure 17). In particular, when the stiffness is lowered by 1×10^{-4} times, the maximum impact fore will be significantly reduced to 13.3 times. Apparent, the stiffness reducing is importance for the rock-shed slab.

(4) Thickness of the dissipation cushion

Another design guideline is to use a dissipation cushion on the rock-shed. The results show only a slight reduction in the maximum impact force if the thickness of the dissipation cushions is increase

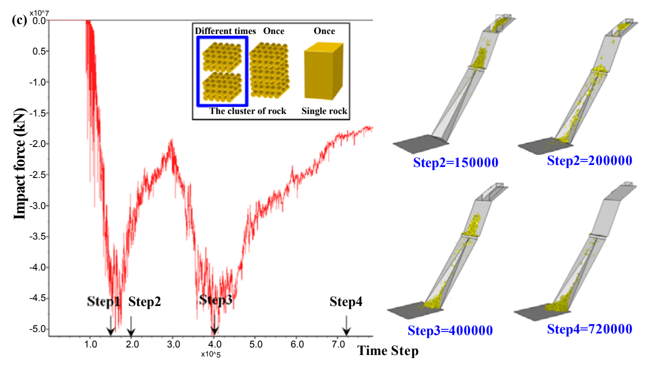

Figure 13c: Impact processes in case study simulated by SCSF models.

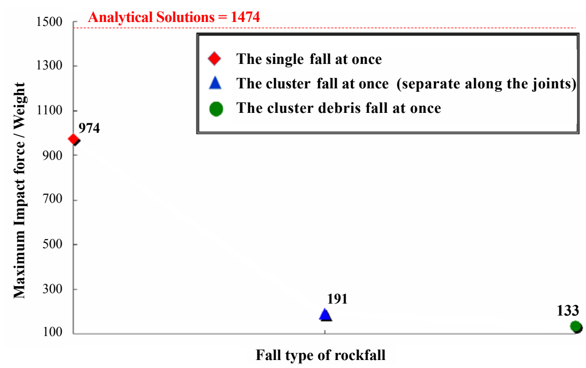

Figure 14: Relationship of maximum impact force/weight and fall type.

Simulation items \ Discussion items			Single fall (Fmax/Weight)	Cluster fall (Fmax/Weight)	Sub-cluster cluster in sequence fall (Fmax/Weight)	Remarks
Joint spacing (m)	1			185		
	4			191		
	7			333		
	10			833		
Type of rockfall	Single fall		974			Joint spacing: 4 m
	Sub-cluster in sequence fall	B_1		191		
		B_2			175	
		B_3			157	
		B_4			142	
		B_5			140	
	Cluster in sequence fall	C_1		133		Particle size: 0.5~1 m
		C_2			103	
		C_3			103	
		C_4			101	
		C_5			98	
Stiffness of the top slab (kN/m)	1E+5			19.5		Joint spacing: 4 m
	1E+6			153		
	1E+7			255		
	1E+9			260		
Depth of dissipation cushion (m)	1			249		Joint spacing: 4 m Particle size of cushion: 0.5 m
	3			241		
	5			240		
	7			220		
	9			219		
Fmax: Maximum impact force (kN); Weight: 420000 kN.						

Table 5: Results of the case study simulation by PFC models.

Citation: Lo CM, Lee CF, Lin ML (2016) Consideration of the Maximum Impact Force Design for the Rock-Shed Slab. J Geogr Nat Disast 6: 169. doi:10.4172/2167-0587.1000169

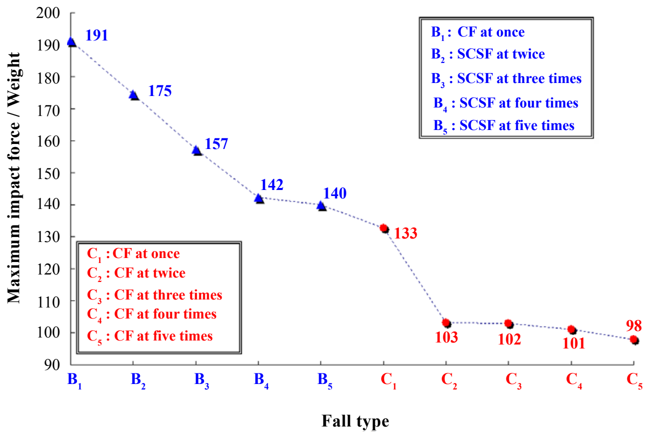

Figure 15: Relationship of maximum impact force/weight and sub-cluster in sequence of fall type.

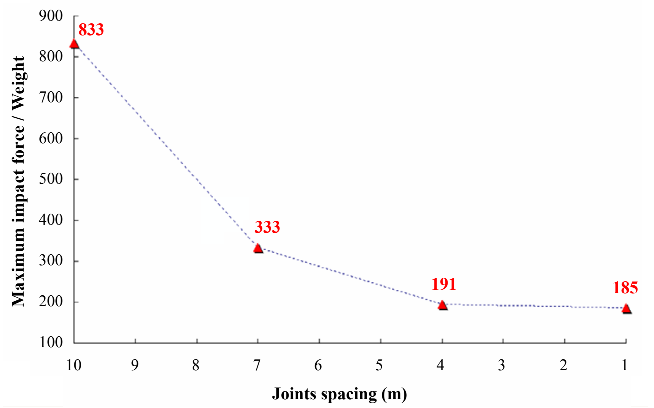

Figure 16: Relationship of maximum impact force/weight and joint spacing.

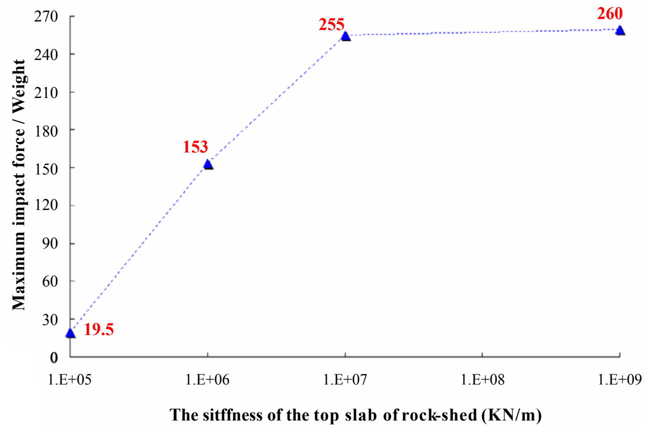

Figure 17: Relationship of maximum impact force/weight and stiffness of top slab.

(Figure 18). Although increasing the dissipation cushion are not significantly efficiency with respect to the entire structure stiffness reduced for reducing maximum force. However, application of used dissipation cushion layer in rock shed can cushion rock falls impact and effectively reduce the maximum impact force. Dissipation cushion layer thickened can slightly improve reduce stiffness and increase energy absorption capacity for the whole structure of the rock-shed [17-20].

Discussion and Conclusions

This paper focuses on the estimation of the maximum impact force on a rock-shed by clusters of rock falls. The findings are summarized as follows:

(1) A comparison of the results obtained from the analytical solution, physical modeling and numerical modeling shows that the major factors influencing the maximum impact force of a collision are the mass and drop height of the rock falls as well as the contact stiffness of the roof slab material. Furthermore, the volume and type of rock falls, the surrounding terrain and the stiffness of the material of the top slab are the main factors of concern when designing a rock-shed. This study offers guidelines for the preliminary design of rock-sheds for protection from rock falls.

(2) The new structurally dissipating rock-sheds (SDR) (Delhomme, 2005 and 2007) are recommended. This type of rock-shed includes extra flexible steel pillars between the top slab and the columns, which decreases the stiffness of contact during rock falls collisions and thus effectively reduces the maximum impact force and damage. Our simulation results (the stiffness decreases part) support this engineering design, when the structure stiffness decreases, the maximum impact force by rock falls also are decreased (Figure 17). Therefore, reducing the stiffness of the whole structure of the rock-shed is the key method for avoid impact failure risk by rock falls.

(3) Rock shed is commonly used in traffic disaster protection. In order to improve rock shed performance, impact cushion and energy absorption measures are usually adopted. It is important to build impact-resistant, durable and efficient auxiliary energy dissipation cushions. Figure 18 shows that the dissipation cushion is increased by 8 m, the maximum impact fore will be reduced to 12%. In practical engineering application, dissipation cushion layer can be set up with multilayer and filled with polyurethane foam, polystyrene, low-density industrial waste, or other lightweight materials with a cell structure in order to improve the rigidity and energy absorption capacity of cushion layer (Sun et al., 2016). In addition, careful consideration of the thickness of the cushions is indispensable, and the repose angle of field talus deposit should also be taken into account for appropriate design of the slope of the top slab.

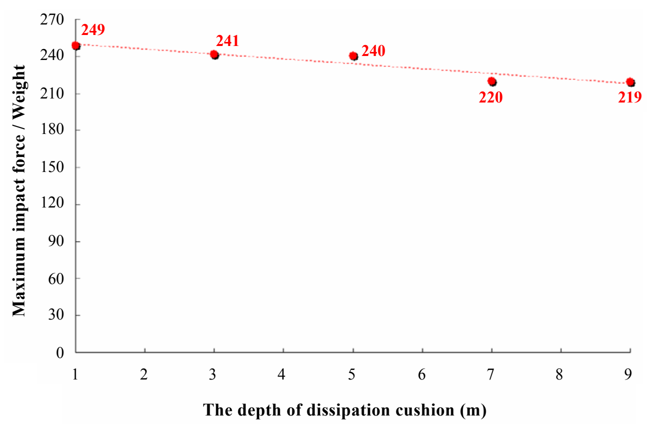

Figure 18: Relationship of maximum impact force/weight and depth of dissipation cushion.

(4) Rocks falling from heights of 50 m to 100 m with volumes of 1000 m^3 to 50000 m^3 are common on the Central Cross-island Highway. The maximum impact force of potential rock falls can be estimated and compared to the capacity of the rock-shed. It may sometimes be appropriate to blast the rock mass to ensure it falls in sequence. This measure would diminish the rock size and the contact stiffness and thus effectively reduce the maximum impact force of clusters of rock falls.

(5) This study provides valuable insight into the quantification of the maximum impact force of clusters of rock falls. Nevertheless, there are a few limitations. The first concerns the damping effects, which are not considered in this system. The second concerns the behavior of a breach in the rock, which is not considered in the interaction of rock falls collision. The influences of the shape of the falling rock and the contact modes have not yet been considered.

References

1. Sébastien H, Laurent D, Frédéric D (2003) Modeling of reinforced concrete structures subjected to impacts by the discrete element method. 16th ASCE Engineering Mechanics Conference, Seattle, University of Washington 1-14.
2. Delhomme F, Mommessin M, Mougin JP, Perrotin P (2005) Behavior of a structurally dissipating rock-shed: experimental analysis and study of punching effects. International Journal of Solids and Structures 42: 4204-4219.
3. Philippe BR, Yehya T, Laurent D, Jacky M (2003) Finite element modeling of concrete protection structures submitted to rock impacts. 16th ASCE Engineering Mechanics Conference, Seattle, University of Washington 1-12.
4. Ebeltoft R, Larsen JO, Nordal S (2006) Instrumentation of buried flexible culvert subjected to rock fall loading. Joint International Conference on Computing and Decision Marking in Civil and Building Engineering 95-103.
5. Chuman Y, Mimura K, Kaizu K, Tanimura S (1997) A sensing block method for measuring impact force generated at a contact part: International Journal of Impact Engineering 19: 165-174.
6. Okura Y, Kitahara H, Sammori T, Kawanami A (2000) The effect of rockfall volume on runout distance. Journal of Engineering Geology 58: 109-124.
7. Itasca Cons Group (1999) PFC3D (Particle Flow Code in 3 Dimension) Version 3.0, Minneapolis 3-1-3-84.
8. Potyondy DO, Cundall PA (2004) A bonded-particle model for rock. International Journal of Rock Mechanics Mining Sciences 41: 1239-1364.
9. Cundall PA, Strack OD (1979) A discrete numerical model for granular assemblies: Geotechnique 29: 47-65.
10. Giani GP (1992) Rock slope stability analysis. Balkema AA, Rotterdam p: 361.
11. Flageollet JC, Weber D (1996) Fall. In: Dikau R, Brunsden D, Schrott L, Ibsen M (eds.) Landslide recognition. Identification, movement and causes. John Wiley & Sons, Chichester pp: 13-28.
12. Chang YL, Chu BL, Li SS (2003) Numerical simulation of gravel deposits using multi-circle granule model: Journal of the Chinese Institute of Engineering 26: 681-694.
13. Daudeville L, Donzé FV, Mazars J (2005) Impacts on concrete structures: from the local analysis to the structural behaviour. International Conference on Computational Plasticity 8: 1-4.
14. Delhomme F, Mommessin M, Mougin JP, Perrotin P (2007) Simulation of a block impacting a reinforced concrete slab with a finite element model and a mass-spring system. Engineering Structures 29: 2844-2852.
15. Sun JH, Chu ZJ, Liu YF, Luo WM, Wang M (2016) Performance of Used Tire Cushion Layer under Rockfall Impact. Shock and Vibration 10: 1-10.
16. Lo CM, Chang KJ (2015) The Maximum Impact Force from a Rock-fall for Rock-Shed Slab Design. Journal of Chinese Soil and Water Conservation 46: 197-204.
17. Magnier SA, Donze FV (1998) Numerical simulations of impacts using a discrete element method. Mechanics of Conhesive-Frictional Materials 3: 257-276.
18. Mougin JP, Perrotin P, Mommessin M, Jean T, Amen A (2005) Rock fall impact on reinforced concrete slab: an experimental approach. International Journal of Impact Engineering 31: 169-183.
19. Shi LP, Huang TH, Hung JJ (1995) A study on the uniaxial compression behaviors and acoustic emission characteristics of rocks in Taiwan. The 8th International Congress on Rock Mechanics, Tokyo Japan 25-30.
20. Wen L, Benno MN (2000) A mechanical model to determine the influence of masses and mass distribution on the impact force during running. Journal of Biomechanics 33: 219-224.